

# Effect of Amino Acid Replacements on the Structural Stability of Fish Myoglobin

Nobuhiko Ueki\* and Yoshihiro Ochiai†

Laboratory of Aquatic Molecular Biology and Biotechnology, Graduate School of Agricultural and Life Sciences, The University of Tokyo, Bunkyo, Tokyo 113-8657

Received June 7, 2006; accepted September 14, 2006

**Structural stabilities of myoglobin (Mb) from several fish (scombridae) species differ significantly, although their amino acid sequence identity is very high (>95%), suggesting that only a few substitutions greatly affect the stability of Mb. Accordingly, recombinant Mbs with point mutation(s) derived from bigeye tuna Mb cDNA were expressed as GST-fusion proteins in the soluble fractions of *Escherichia coli*. After removal of the GST segment, the stability of five mutants, namely, P13A, I21M, V57I, A62G, and I21M/V57I, together with the wild type (WT) were investigated, taking temperature dependency of  $\alpha$ -helical content and denaturant concentration dependency of Soret band absorbance as parameters. As a result, the stability of P13A against denaturants and its  $\alpha$ -helical content at 10°C was found to be the highest among the mutants, whereas those of A62G were the lowest. The stabilities of V57I and I21M/V57I were higher than that of WT, though that of I21M was nearly the same as WT. These findings suggest that the structural stability of fish Mb is tuned up only by the substitutions of a few amino acid residues located in the  $\alpha$ -helical segments forming the hydrophobic heme pocket.**

**Key words:** fish, mutant, myoglobin, stability, tuna.

Abbreviations: Mb, myoglobin; MALDI-TOF, matrix-assisted laser desorption/ionization-time of flight; metMb, metmyoglobin; CD, circular dichroism; GdnHCl, guanidine hydrochloride; GST, glutathione S-transferase; PCR, polymerase chain reaction; SDS-PAGE, sodium dodecyl sulfate–polyacrylamide gel electrophoresis; WT, wild type.

Myoglobin (Mb) is the globular heme protein whose molecular weight is generally 15,000–17,000. Mb plays a role in oxygen storage in muscle by virtue of coordinate bond between the imidazole group of distal His and oxygen (1). The heme is held in hydrophobic "heme pocket," and binds imidazole group of proximal His directly and through the coordinate bond. Interaction of heme and globin, particularly proximal and distal His residues at the heme pocket, is important for stabilization. This protein consists of eight  $\alpha$ -helical segments designated A through H from the N terminus (2, 3). As for fish, Mb is widely distributed in muscle, particularly in slow skeletal (dark) and cardiac muscles (4). Fish Mb lacks D helix as has been revealed in that of yellowfin tuna *Thunnus albacares* (5). Metmyoglobin (metMb) is accumulated at post mortem stage by oxidation of heme iron due to inactivation of endogenous Mb reducing system, and as a result, color of muscle turns brown. Previous studies showed that metMb is more susceptible to denaturation compared with the other forms, and progression of discoloration is accelerated by freezing and thawing due to the perturbation of globin structure (6, 7).

So far, site-directed mutagenesis has been applied to the investigation on stability of apo Mb, molten globule intermediate, heme binding, and intramolecular electron

transfer (8–11). Smerdon *et al.* (12) reported that heme dissociation from porcine Mb was promoted by replacement of Ser92 with Leu or Ala. The mutations of distal His64, Val 68, and Arg45 also affected heme dissociation profile (13). These results suggested that such amino acid residues as are involved in the hydrophobicity of heme pocket, are the important factors for stability of Mb. Luo *et al.* (14) reported that the features of apo-form intermediate of sperm whale Mb were affected by mutation of Gln8 or Glu109. Moreover, Musto *et al.* (15) revealed that stability of sea hare Mb intermediate was decreased by replacement of Trp130 with Tyr (the residue corresponding to Trp131 of sperm whale Mb) which is important for the packing of helices A, G and H observed at the initial state of folding. Although helix F of sperm whale apo Mb was flexible due to the presence of Pro at the center of this segment, the  $\alpha$ -helical structure was reinforced by replacement of this Pro with Ala, thus giving a rigid tertiary structure as demonstrated by resistance against proteolysis (16). It is thus clear that structural properties of Mb dramatically change by substitution(s) of a few key amino acid residue(s).

Many species in scombridae, especially tunas, have acclimated to fast cruising. The high amount (~100 mg/g) of Mbs present in their skeletal muscles (not only in slow skeletal muscle but also in fast skeletal muscle) supports such unique locomotion activity of these species. In the previous studies (17, 18), it was revealed that structural stabilities of scombridae fish Mbs clearly differed depending on species, although the amino acid sequence identities were very high. Especially, there were only two substitutions between bigeye tuna *Thunnus obesus*

\*Present address: Laboratory of Peptide Biosignal Engineering, Mitsubishi Kagaku Institute of Life Sciences, Machida, Tokyo 195-8511.

†To whom correspondence should be addressed: Phone/Fax: +81-3-5841-7521, E-mail: aochiai@mail.ecc.u-tokyo.ac.jp

and yellowfin tuna Mbs despite clear difference in thermostability between them. It follows that the residues responsible for stabilization (or destabilization) of this protein can be pinpointed for Mbs from this fish group.

In the present study, in order to elucidate the amino acid residue(s) that substantiates the structural stability difference among tuna Mbs, five Mb mutants, namely, those of P13A, I21M, V57I, A62G, and I21M/V57I, were elaborated based on the sequence of bigeye tuna Mb. The mutation sites were determined due to the following reasons. P13A is the substitution present specifically to skipjack tuna *Katsuwonus pelamis* Mb whose stability was the highest among all the scombridae fish Mbs examined (18). A62G is the specific mutation in bullet tuna *Auxis rochei* Mb whose stability was the lowest among all the scombridae fish Mbs examined (18). I21M and V57I were the only two substitutions between bigeye tuna and yellowfin tuna Mbs. These mutant Mbs were compared based on their temperature dependency of  $\alpha$ -helical contents and effect of denaturants on Soret band absorbance.

#### MATERIALS AND METHODS

**Construction and Purification of Mutant Mb**—Site-directed mutagenesis was performed using polymerase chain reaction (PCR) according to Landt *et al.* (9). pGEX-2T plasmid containing bigeye tuna wild type (WT) Mb cDNA was constructed as reported previously (17). PCR was initiated by adding 1 ng of pGEX-2T plasmid as a template to 100  $\mu$ l of a reaction mixture containing 10  $\mu$ l of 10 $\times$  *pfu* buffer, 50 mM dNTP mixture, 100 pmol each of primers, namely a mutagenic primer (Fig. 1 [1], Table 1) and 5' primer KuMeEx-F (Fig. 1 [2]), and 1 U of

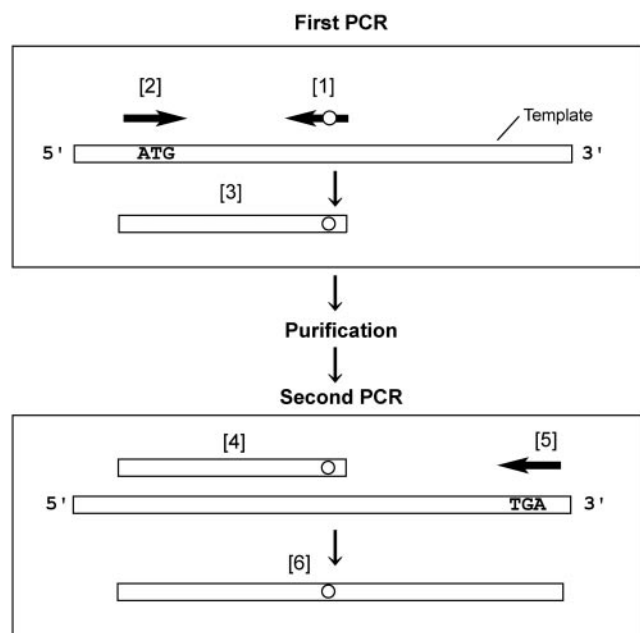


Fig. 1. Schematic representation of the PCR mutagenesis method. In the first PCR, the mutagenesis primer [1] and the 5' primer [2] were used, yielding a product [3]. After purification, the second PCR was performed using the mutagenesis long primer [4] and 3' primer [5], yielding a mutated fragment [6]. The open circle indicates the mutation site.

cloned *pfu* DNA polymerase. PCR consisted of initiating denaturation step at 94°C for 5 min, followed by 30 cycles of denaturation at 94°C for 60 s, annealing at 45°C for 60 s, and extension at 72°C for 45 s. The final extension step was performed at 72°C for 5 min. The 5' primer [2], which hinders precise second PCR, was removed from the PCR products obtained by the first PCR. After treatment with Exo-SAP-IT (Amersham Biosciences, Piscataway, NJ, USA), the fragment was extracted with phenol/chloroform, and precipitated with ethanol. The purified fragment [3] was used as a 5' mutagenic primer [4] for the second PCR. The second PCR was performed under the conditions for the first PCR step with the following modifications: the concentration of dNTP was 200  $\mu$ M and that of the 3' primer [5] was 1  $\mu$ M. Thus, the PCR product [6] was obtained. The PCR products were digested with *Bam*HI and *Sma*I, and subcloned into a pGEX-2T vector. Nucleotide sequences were determined by an ABI PRISM 3100 DNA sequencer (Applied Biosystems, Foster City, CA, USA) using BigDye Terminator Cycle Sequencing Kit Version 3 (Applied Biosystems).

After *Escherichia coli* BL21 (DE3) pLysS (Novagen, San Diego, CA, USA) was transformed by the pGEX-2T vector (Amersham), expression of recombinant Mb was carried out. Namely, the *E. coli* strain harboring recombinant Mb plasmid was cultured at 30°C in 1 l of LB medium containing 50  $\mu$ g/ml ampicillin for 3 h until the absorbance at 600 nm reached around 0.5. Subsequently, 20 mg of hemin (Sigma-Aldrich, St. Louis, MO, USA) was added, and expression was induced with 1 mM isopropyl- $\beta$ -D-thiogalactopyranoside (IPTG) for 6 h. After centrifugation at 3,000  $\times$ g for 15 min at 4°C, the precipitate was subjected to sonication in 50 mM Tris-HCl (pH 8.0) containing 150 mM NaCl, 1 mM EDTA, and 1 mM dithiothreitol on ice. After addition of 10% (w/v) Triton X-100, the sonicate was subjected to ultracentrifugation at 12,000  $\times$ g for 30 min at 4°C. The supernatant, after checking the expression of glutathione *S*-transferase (GST) fusion protein, was filtered through a 0.45  $\mu$ m nitrocellulose filter (Millipore, Billerica, MA, USA).

The cell extract was purified with a GSTrap column (Amersham) as follows. Soluble fraction was absorbed on a GSTrap column equilibrated with PBS (10 mM NaHPO<sub>4</sub>, 1.8 mM KH<sub>2</sub>PO<sub>4</sub>, 140 mM NaCl, and 2.7 mM KCl, pH 7.3) and washed with 4 column volumes of the same buffer to remove unabsorbed substances. Then, GST fusion protein was eluted with 50 mM Tris-HCl (pH 8.0) containing 10 mM reduced glutathione. The fusion protein was digested with 10 units/mg of thrombin for 10 h at 25°C to excise the GST portion from Mb. To remove the excised GST, the digest was applied to the GSTrap column again. Finally, thrombin was removed by a batch method using a Benzamidine Sepharose 6B column (Amersham) equilibrated with 25 mM Na-phosphate (pH 8.0) containing

Table 1. Sequence of primers used for PCR.

Primer	Sequence
P13A	5'-CCTCCACTGCACCCCAAC-3'
I21M	5'-GGCCTCCCATGGTGGTGTAG-3'
V57I	5'-CCATGAGCAGAAATAGCTGCG-3'
A62G	5'-GCACAGTGCCACCATGAGC-3'

0.5 M NaCl, and the recombinant protein (apo form) was obtained in the unabsorbed fraction.

To obtain holo Mb, the apo Mb was further treated with hemin. Apo Mb was incubated with hemin at the molar ratio of Mb:hemin = 1:2 at 4°C for 30 min. The mixture was then dialyzed against the stepwise decreasing concentrations of urea from 6 to 0 M. Remaining apo form was removed by ultracentrifugation at 90,000 × *g* for 20 min at 4°C. Introduction of hemin to globin was verified by Soret band absorbance at 405 nm.

**Molecular Mass Measurement**—After desalting with ODS resin (ZipTip<sub>C18</sub>; Millipore), molecular mass of Mb was measured by matrix-assisted laser desorption/ionization-time of flight (MALDI-TOF) mass spectrometry using a Voyager DE-STR (Applied Biosystems). Sinapinic acid (Sigma-Aldrich) was used as a matrix. Then actual values of molecular mass were compared with theoretical values calculated by MS-digest program of ProteinProspector on UCSF Mass Spectrometry Facility.

**Temperature Dependency of  $\alpha$ -Helical Contents**—Changes in the  $\alpha$ -helical contents of recombinant Mbs were measured by circular dichroism (CD), and compared with those of native Mbs. CD measurement was carried out with a J-700W spectropolarimeter (JASCO, Tokyo, Japan) using a 0.2 mm water-jacketed cylindrical cell in the temperature range of 10–85°C with the increment of 5°C (10–40°C) or 2.5°C (40–85°C). The data were collected 10 min after the temperature of the cell reached the preset value. Wavelength for measurement was in the range of 240–195 nm. The determination of  $\alpha$ -helical content was performed according to Yang *et al.* (19) with 200  $\mu$ g/ml of Mb in 10 mM Na-phosphate (pH 7.0) containing 150 mM KCl.

**Effect of Denaturant Concentration on Soret Band Absorbance**—Soret band absorbance of Mb was measured as an index of denaturation. Concentrations of urea and guanidine hydrochloride (GdnHCl) were adjusted in the range of 0–6.49 and 0–2.5 M, respectively, by adding 30  $\mu$ l aliquots of 10 M urea and 20  $\mu$ l aliquots of 6 M GdnHCl for 700 and 600  $\mu$ l, respectively, to Mb solution in 10 mM Na-phosphate (pH 7.0) containing 150 mM KCl. After incubation of the mixture at 25°C for 5 min, the absorbance at 405 nm was measured. It was preliminarily confirmed that the denaturing condition was sufficient for recombinant fish Mbs to reach the structural equilibrium due to their thermal lability (20). Protein concentration was in the range of 0.1–0.2 mg/ml. The measurements were performed in triplicate.

Free energy for denaturation ( $\Delta G_D$ ) was calculated from the following equations (21),

$$K_D = (E_N - E_{\text{obs}})/(E_{\text{obs}} - E_D)$$

where  $K_D$  is the equilibrium constant in denaturation,  $E_N$  and  $E_D$  stand for the molar extinction coefficients of protein in the native and denatured states, respectively, and  $E_{\text{obs}}$  is the observed molar extinction coefficient of the protein transition between the native and denatured states.

$$\Delta G_D = -RT \ln K_D$$

where  $R$  is the gas constant (1.987 cal·deg<sup>-1</sup>·mol<sup>-1</sup>) and  $T$  is the absolute temperature. The intrinsic value for  $\Delta G_D$  of Mb was obtained by using the linear correlation between

the value of  $\Delta G_D$  and denaturant concentration. Therefore, the free energy stability of protein in the absence of denaturant was calculated by the equation,

$$\Delta G_{\text{H}_2\text{O}}^0 = \Delta G_D + mC$$

where  $C$  represents the molar concentration of the denaturant, and  $m$  the slope of regression line. Stability of Mb was evaluated by the denaturant molarity at the transition midpoint ( $C_m$ ).

**Prediction of Hydropathy and Helical Propensity**—Hydropathy was calculated by using the algorithm of Kyte and Doolittle (22) based on the deduced amino acid sequence. Helical propensity was calculated by using the AGADIR algorithm of Munoz and Serrano (23) based on the deduced amino acid sequences with the N-terminal Ala being acetylated.

**Other Experimental Procedures**—Alignment of amino acid sequences of bigeye tuna Mb with those of other scombridae fish species was performed using the ClustalW program (24). DDBJ/EMBL/GenBank accession numbers for the cited sequences are as follows; bigeye tuna, AB104433 (17); bluefin tuna *Thunnus thynnus*, AF291831 (25); yellowfin tuna, AF291838 (25); bullet tuna, AB154423 (18); and skipjack tuna, AF291837 (25). Purity of bigeye tuna Mb mutants was estimated by sodium dodecyl sulfate–polyacrylamide gel electrophoresis (SDS-PAGE). SDS-PAGE was performed by the method of Laemmli (26) using 17.5% gel. The standard molecular weight marker kit used was SDS-7 (Sigma-Aldrich). Protein concentration was determined by BCA Protein Assay Kit (Pierce, Rockford, IL, USA), according to the manufacturer's protocol using horse Mb (Sigma-Aldrich) as a standard.

## RESULTS

**Construction and Purification of Mb Mutants**—Scombridae fish Mbs consisted of 146–147 amino acids. The amino acid sequences of Mbs from five fish species were aligned in comparison with that of bigeye tuna (Fig. 2). One gap was recognized in the C-E loop of skipjack tuna Mb. The figure shows the mutation sites (boldfaced in the figure) in recombinant Mbs. These residues were targeted because they are the outstanding differences between the stable and unstable Mbs (17). All the mutation sites were located in the helices A, B and E. The mutants were obtained as GST fusion proteins, but the GST portion could be completely removed (20). Figure 3 shows the SDS-PAGE patterns of purified Mb mutants. Clear single bands of about 15 kDa were recognized for all the mutants. Furthermore, any peaks of impurity were not observed by MALDI-TOF mass spectrometry (data not shown). Actual values of mass-to-charge ratio ( $m/z$ ) of Mb mutants were very close to the theoretical values, which included the additional Gly and Ser to the N-terminus of mutant Mbs (Table 2).

**Temperature Dependency of  $\alpha$ -Helical Contents**—The molar ellipticity at 222 nm ( $[\theta]_{222}$ ) increased as the temperature was raised (Fig. 4).  $\alpha$ -Helical content of mutant A62G at 10°C was the lowest (31.5%), while that of P13A was the highest (38.8%) among the mutants. As for I21M, V57I, and I21M/V57I, clear differences were not recognized

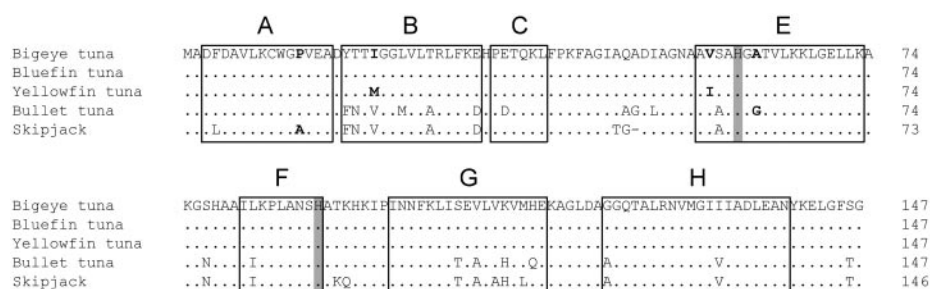


Fig. 2. Alignment of amino acid sequences of bigeye tuna Mb with those of other scombridae fish species. Amino acid residues identical to those of bigeye tuna Mb are indicated with dots, and the gaps are indicated by dashes. Boxes contain the  $\alpha$ -helical segments A, B, C, E, H, G, and H. Segment D is missing in fish Mbs. Heme-binding histidine residues are shaded. The sites of mutation are indicated by bold-faced letters.

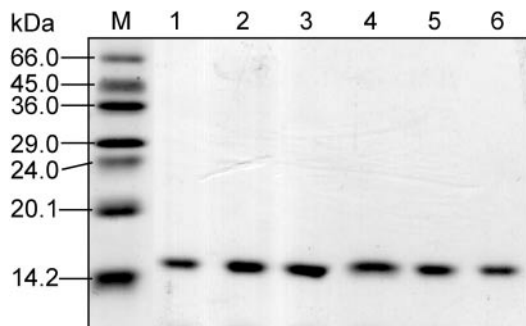


Fig. 3. SDS-PAGE patterns of purified bigeye tuna Mb mutants. M, markers; 1, wild type; 2, mutant P13A; 3, I21M; 4, V57I; 5, A62G; 6, I21M/V57I. 17.5% gel. Five micrograms of Mb was applied to each lane.

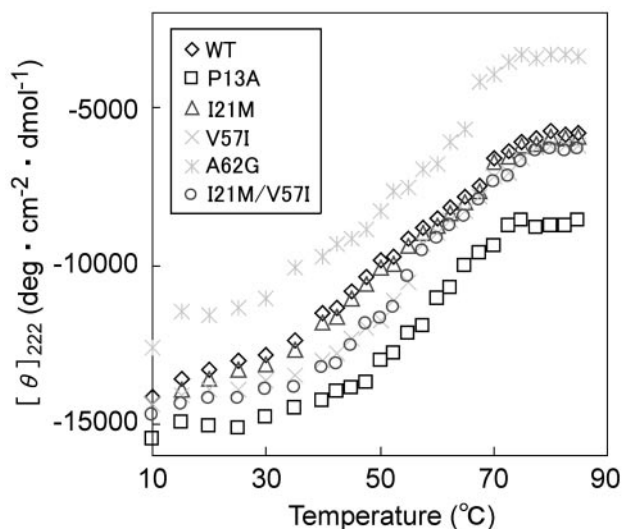


Fig. 4. Effects of temperature on the mean residue ellipticity at 222 nm of bigeye tuna Mb mutants. CD spectrometry was performed in 10 mM Na-phosphate (pH 7.0) containing 0.15 M KCl in the temperature range of 10–85°C with the increment of 5°C (10–40°C) or 2.5°C (40–85°C). Protein concentration was adjusted to 200 mg/ml. WT, wild type.

(36.3, 36.0, and 36.8%, respectively) when compared with that of WT (35.5%). However, in the temperature range of 35–52.5°C,  $\alpha$ -helical contents of V57I and I21M/V57I were higher than that of WT. Irrespective of temperature range,

Table 2. Actual and theoretical mass of bigeye tuna Mb mutants.

Mutant	Actual value ( $m/z$ ) <sup>a</sup>	Theoretical value ( $m/z$ ) <sup>b</sup>
WT	15,769.2	15,772.5
P13A	15,741.8	15,746.5
I21M	15,790.2	15,790.6
V57I	15,790.4	15,786.5
A62G	15,760.2	15,758.5
I21M/V57I	15,806.2	15,804.6

<sup>a</sup>Actual values were measured by MALDI-TOF mass spectrometry

<sup>b</sup>Theoretical values were calculated by MS-digest program of ProteinProspector on UCSF Mass Spectrometry Facility based on the deduced amino acid sequences of bigeye tuna Mb mutants, respectively.

the helical content of P13A was clearly higher and that of mutant A62G was lower than WT counterparts. All the proteins were denatured irreversibly through the first heat treatment (data not shown) due to aggregation (17). Therefore, thermodynamic calculation based on CD spectra was given up. Differential scanning calorimetry (DSC) was not carried out in the present study due to the same reason. However,  $\alpha$ -helical contents represent the overall structural changes of Mb molecule, because the helical regions are present along almost the entire molecule as shown in Fig. 2.

**Effect of Denaturants on Soret Band Absorbance**—Dramatic decline of Soret band absorbance was observed in the urea concentration range of 4.1–6.0 M. The stabilities of P13A, V57I, and I21M/V57I against urea were high ( $-\Delta G_{\text{H}_2\text{O}}^0 = 4.78, 3.88, \text{ and } 3.90 \text{ kcal/mol}$ , respectively), and the stability of A62G was low (2.76 kcal/mol) when compared with that of WT (3.74 kcal/mol) (Fig. 5 and Table 3). Especially, the stability of P13A was the highest, and that of A62G was the lowest among all the mutants examined. In the case of GdnHCl, Soret band absorbances of the mutants were steeply decreased in the concentration range of 1.2–2.1 M, and the denaturation profiles were very similar to those in the presence of urea (Fig. 6 and Table 4).

**Prediction of Hydropathy and Helical Propensity**—Hydropathy and helical propensity of bigeye tuna Mb were affected by amino acid replacement (Fig. 7). Hydrophobicities in the vicinity of mutation sites were increased by mutation of P13A, and were decreased by mutations such as I21M and A62G, while hydropathy score of V57I was similar to that of WT. Helical propensities in the vicinity of mutation sites were slightly increased by mutations

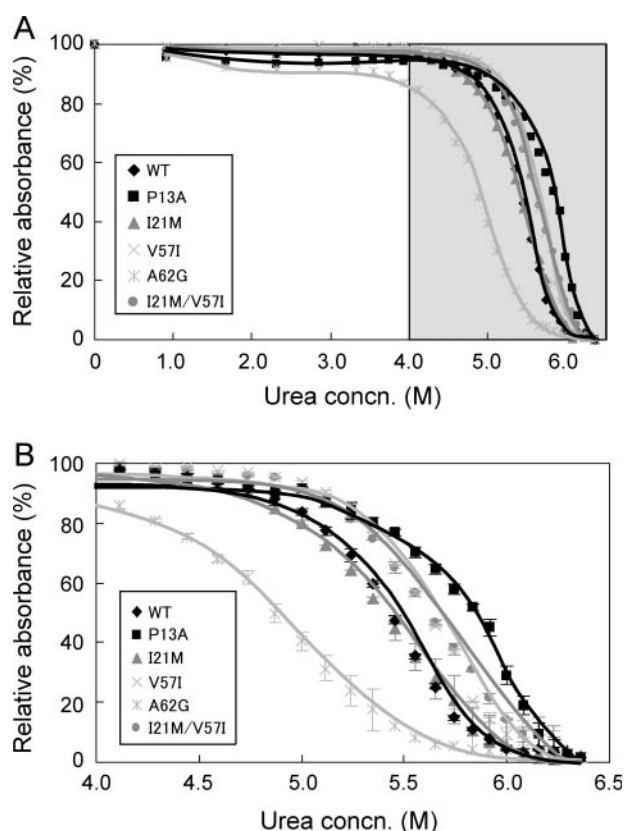


Fig. 5. Effect of urea on Soret band absorbance of bigeye tuna Mb mutants. The shaded area of panel A was magnified, and indicated in panel B. Absorbance at 405 nm was measured in 10 mM Na-phosphate (pH 7.0) containing 0.15 M KCl. Approximate curves were indicated in black for WT and mutant P13A, in gray for I21M and I21M/V57I, and in light gray for V57I and A62G. Protein concentration was 0.1–0.2 mg/ml. WT, wild type.

Table 3. Standard free energy of unfolding ( $-\Delta G_{H_2O}$ ) as determined by using urea as a denaturant and transition midpoint ( $C_m$ ) of bigeye tuna Mb mutants.

Mutant	$-\Delta G_{H_2O}$ (kcal/mol)	$C_m$ (M)
WT	$3.74 \pm 0.04^a$	$5.37 \pm 0.02^a$
P13A	$4.78 \pm 0.06$	$5.76 \pm 0.05$
I21M	$3.67 \pm 0.02$	$5.35 \pm 0.14$
V57I	$3.88 \pm 0.03$	$5.57 \pm 0.01$
A62G	$2.76 \pm 0.03$	$4.81 \pm 0.20$
I21M/V57I	$3.90 \pm 0.02$	$5.59 \pm 0.05$

<sup>a</sup>Mean  $\pm$  SD for triplicate determinations.

of P13A, I21M, and V57I, and were decreased by mutation of A62G.

## DISCUSSION

In the previous studies (17, 18, 20), it was established that tuna Mbs clearly differ in thermal stability despite the high amino acid sequence identity (>84%). Namely, the  $T_m$  values obtained by DSC analyses were 75.7, 78.6, 78.2, 71.7, and 79.9°C for Mbs from bigeye tuna, bluefin tuna, yellowfin tuna, bullet tuna and skipjack tuna, respectively.

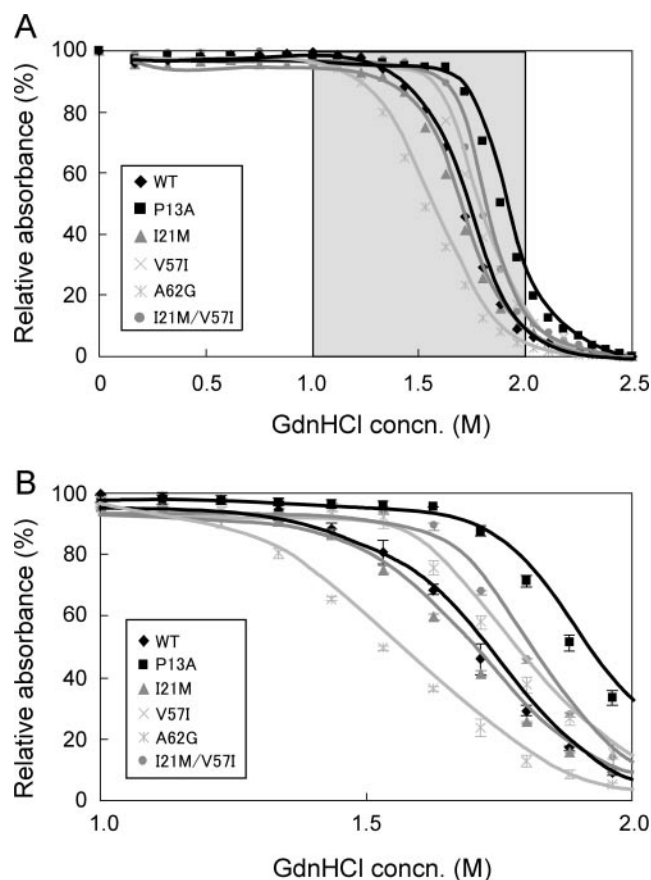


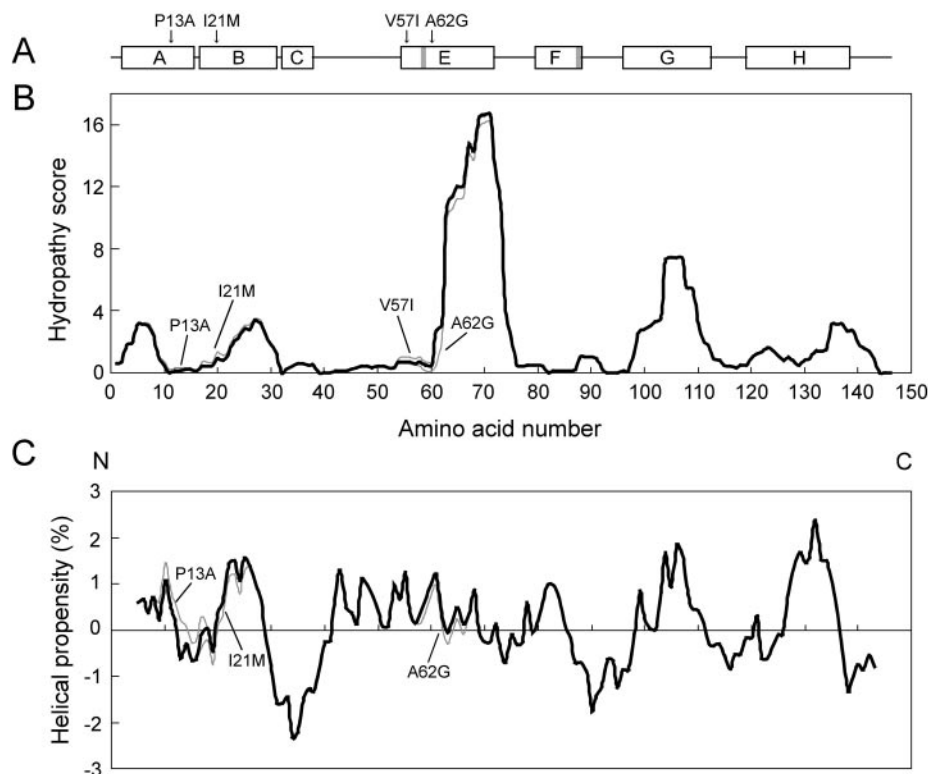
Fig. 6. Effect of guanidine HCl on Soret band absorbance of bigeye tuna Mb mutants. The shaded area of panel A was magnified, and indicated in panel B. Absorbance at 405 nm was measured in 10 mM Na-phosphate (pH 7.0) containing 0.15 M KCl. Approximate curves were indicated in black for wild type and mutant P13A, in gray for mutants I21M and I21M/V57I, and in light gray for mutants V57I and A62G. Protein concentration was 0.1–0.2 mg/ml. WT, wild type.

Table 4. Standard free energy of unfolding ( $-\Delta G_{H_2O}$ ) as determined by using GdnHCl as a denaturant and transition midpoint ( $C_m$ ) of bigeye tuna Mb mutants.

Mutant	$-\Delta G_{H_2O}$ (kcal/mol)	$C_m$ (M)
WT	$2.37 \pm 0.02^a$	$1.69 \pm 0.02^a$
P13A	$2.84 \pm 0.04$	$1.91 \pm 0.01$
I21M	$2.35 \pm 0.03$	$1.67 \pm 0.01$
V57I	$2.53 \pm 0.06$	$1.79 \pm 0.02$
A62G	$2.10 \pm 0.01$	$1.53 \pm 0.01$
I21M/V57I	$2.60 \pm 0.05$	$1.81 \pm 0.01$

<sup>a</sup>Mean  $\pm$  SD for triplicate determinations.

In the present study, effects of amino acid substitution on the stability of bigeye tuna Mb were investigated. Hemin was incorporated to the mutant Mbs to assist proper folding, because the helix F is disordered by removal of heme (27). It is already established that the helices A, G, and H are already structured forming a hydrophobic core in the molten globule state, and the helices B and E are also involved in the core formation in apo Mb (28). Though it is known that the intermediate state is nearly as compact as the native apo Mb (29, 30), the Soret band absorbance and



**Fig. 7. Changes of hydropathy and helical propensity of bigeye tuna Mb by mutation.** A: structure of Mb. Boxes and horizontal lines stand for  $\alpha$ -helical segments and intersegment loops (including N- and C-terminal extensions), respectively, and the arrows indicate mutation sites. Proximal and distal His residues are shown by gray boxes. B: hydropathy was calculated by using the algorithm of Kyte and Doolittle (22). C: helical propensities were calculated by using the AGADIR algorithm of Munoz and Serrano (23). Hydropathy and helical propensity of WT are indicated by bold black lines, and those of bigeye tuna Mb mutants are indicated by gray lines.

$\alpha$ -helical content of recombinant Mbs increased as the amount of heme incorporated to the protein as reported previously (20). It is thus likely that addition of heme is effective for appropriate folding of recombinant Mb. On the other hand, absorbance at the Soret band was used as a parameter of structural perturbation by denaturants in this study. The absorbance mainly reflects the heme environment. CD spectrometry around this band was successfully applied to the study on the relation of proximal His and heme (31).

In the case of skipjack tuna Mb, Pro13, located in the helix A of the other scombridae fish Mbs, was absent. Stability of mutant P13A was increased compared with that of WT (Figs. 4, 5, and 6, Tables 3 and 4). Enhanced stability in P13A was reminiscent of the higher stability of skipjack tuna native Mb in comparison with the other scombridae fish Mbs. These results might have been caused by increment in helix propensity around the substituted residues, and thus a more rigid tertiary structure might have been formed. Higher  $\alpha$ -helical contents of P13A compared with that of WT also supported the view (Fig. 4), as in the predicted helical propensity (Fig. 7), though there was a slight difference in the hydropathy score (Fig. 7B). The tertiary structure of skipjack tuna Mb was considered to be rigid and stable. Therefore, Pro13 is considered to be an important substitution for fish Mbs to function properly under low temperature. Incidentally, zebrafish *Danio rerio* Mb (accession No. Q6VN46) and gummy shark *Mustelus antarcticus* Mb also have Pro at this position whereas the corresponding site is occupied by Lys in case of reptiles and mammals. The only exception so far of skipjack tuna Mb might be the result of adaptation to higher swimming speed or higher body temperature. It is well known that Pro to Ala substitution results in stabilization. However, it

is of interest that this fish species adopted the substitution through its molecular evolution of Mb.

It is established that the helix propensity of Ala is very high, whereas that of Pro is very low (32, 33). The helix-breaker Pro is responsible for perturbation of  $\alpha$ -helical structure. Actually, stability of sperm whale apo Mb against proteolytic enzymes was increased by replacement of Pro88 with Ala, facilitating the formation of helix F (16). In this connection, Luo *et al.* (14) reported that sperm whale apo Mb pH 4 folding intermediate was destabilized by introducing the mutations for Pro or Glu in the helices A and G. The results of the present experiment were compatible with these previous reports. It is also reported that mutation in the N-terminus of apo Mb triggers amyloid aggregation (34).

In contrast, stabilities of mutant A62G against denaturants were lower than those of WT (Figs. 5 and 6, Tables 3 and 4). As far as the temperature dependency of  $\alpha$ -helical contents is concerned, that of A62G was lower than that of WT (Fig. 4). These results suggested that stability of Mb was decreased concomitantly with the decline of  $\alpha$ -helical contents due to reduced helix propensity by substitution of Ala with Gly. Moreover, decline of hydrophobicity also reduced the stability of Mb. Ala62 is located in helix E, and very close to distal His60 important for heme binding. This helix E participates in the formation of hydrophobic heme pocket. It is thus suggested that the mutation in such region could affect heme binding, and further the overall stability of Mb. Actually, when Ser92 of sperm whale Mb was substituted with Ala or Leu, heme binding ability became weak and the stability of Mb was decreased (12). Therefore, corresponding Ala62 of bigeye tuna Mb might be crucial for its structural stability. This could be one of the causes for lower stability of bullet tuna Mb which has the

substitution of this site to Gly (18). This species seemed to have adopted this substitution to destabilize its own Mb.

On the other hand, the stabilities of mutants V57I and I21M/V57I against denaturants were higher than that of WT, although the stability of mutant I21M was similar to that of WT (Figs. 5 and 6, Tables 3 and 4). These results suggested that differences in stability between bigeye tuna and yellowfin tuna Mbs are solely attributable to the replacement of Val57 with Ile, but not to that of Ile21 with Met. This might be caused by the difference in locations of these amino acid residues. Namely, while Ile21 of bigeye tuna Mb is located in the helix B, Val57 is located in the helix E, and very close to distal His60 as well as Ala62 described above. Thus, in the case of Val57, it is likely that helical propensity, hydrophobicity, and the bulk of side chains in the heme pocket slightly changed, and stability of Mb was decreased by substitution with Ile.

In the present study, it was revealed that structural stability of bigeye tuna Mb was under control by a slight amino acid substitution, as can be predicted by the mutation studies so far carried out (35). Especially, substitutions of amino acid residue(s) which is located in the  $\alpha$ -helical segments and heme pocket region, greatly affected the tertiary structure of Mb. Stability difference observed between scombridae fish Mbs despite high amino acid sequence identities might be accounted for by the presence or absence of such a few amino acid residues as a consequence of acclimation to locomotion activity and endogenous environment of each species, because cruising speed, habitat water temperature or body temperature differ among the fish species. There are also some minor substitutions among the Mbs of the above five fish species (Fig. 2). The effects of substitutions on the stability of these Mbs are now under investigation.

The authors would like to extend their sincere thanks to Professor S. Watabe, The University of Tokyo, for critically reading the manuscript.

#### REFERENCES

- Phillips, S.E.V. and Schoenborn, B.P. (1981) Neutron diffraction reveals oxygen-histidine hydrogen bond in oxymyoglobin. *Nature* **292**, 81–82
- Kendrew, J.C., Dickerson, R.E., Strandberg, B.E., Hart, R.G., Davies, D.R., Phillips, D.C., and Shore, V.C. (1960) Structure of myoglobin. *Nature* **185**, 422–427
- Vojtechovsky, J., Chu, K., Berendzen, J., Sweet, R.M., and Schlichting, I. (1999) Crystal structures of myoglobin-ligand complexes at near-atomic resolution. *Biophys. J.* **77**, 2153–2174
- Matsuura, F. and Hashimoto, K. (1959) Chemical studies on the red muscle ("chiai") of fishes-X. A new method for determination of myoglobin. *Bull. Jpn. Soc. Sci. Fish.* **24**, 809–815
- Birnbaum, G.I., Evans, S.V., Przybylska, M., and Rose, D.R. (1994) 1.70 Å resolution structure of myoglobin from yellowfin tuna. An example of a myoglobin lacking the D helix. *Acta Cryst.* **D50**, 283–289
- Chow, C.J., Ochiai, Y., Watabe, S., and Hashimoto, K. (1988) Effect of freezing and thawing on the discoloration of tuna meat. *Nippon Suisan Gakkaishi* **54**, 639–648
- Ochiai, Y., Chow, C.J., Watabe, S., and Hashimoto, K. (1988) Evaluation of tuna meat discoloration by Hunter color difference scale. *Nippon Suisan Gakkaishi* **54**, 649–653
- Ho, S.N., Hunt, H.D., Horton, R.M., Pullen, J.K., and Pease, L.R. (1989) Site-directed mutagenesis by overlap extension using polymerase chain reaction. *Gene* **77**, 51–59
- Landt, O., Grunert, H.P., and Hahn, U. (1990) A general method for rapid site-directed mutagenesis using the polymerase chain reaction. *Gene* **96**, 125–128
- Hirota, S., Azuma, K., Fukuba, M., Kuroiwa, S., and Funasaki, N. (2005) Heme reduction by intramolecular electron transfer in cysteine mutant myoglobin under carbon monoxide atmosphere. *Biochemistry* **44**, 10322–10327
- Bourgeois, D., Vallone, B., Arcovito, A., Sciarra, G., Schotte, F., Anfinrud, P.A., and Brunori, M. (2006) Extended subnanosecond structural dynamics of myoglobin revealed by Laue crystallography. *Proc. Natl. Acad. Sci. USA* **103**, 4924–4929
- Smerdon, S.J., Krzywdka, S., Wilkinson, A.J., Brantley, Jr. R.E., Carver, T.E., Hargrove, M.S., and Olsen, J.S. (1993) Serine<sup>92</sup> (F7) contributes to the control of heme reactivity and stability in myoglobin. *Biochemistry* **32**, 5132–5138
- Hargrove, M.S., Singleton, E.W., Quillin, M.L., Ortiz, L.A., Phillips, Jr. G.N., Olsen, J.S., and Mathews, A.J. (1994) His<sup>64</sup>(E7) → Tyr apomyoglobin as a reagent for measuring rates of heme dissociation. *J. Biol. Chem.* **269**, 4207–4214
- Luo, Y., Kay, M.S., and Baldwin, R.L. (1997) Cooperativity of folding of the apomyoglobin pH 4 intermediate studies by glycine and proline mutations. *Nature Struct. Biol.* **4**, 925–930
- Musto, R., Bigotti, M.G., Travaglini-Allocatelli, C., Brunori, M., and Cutruzzola, F. (2004) Folding of *Aplysia limacina* apomyoglobin involves an intermediate in common with other evolutionarily distant globins. *Biochemistry* **43**, 230–236
- Picotti, P., Marabotti, A., Negro, A., Musi, V., Spolaore, B., Zambonin, M., and Fontana, A. (2004) Modulation of structural integrity of helix F in apomyoglobin by single amino acid replacements. *Protein Sci.* **13**, 1572–1585
- Ueki, N. and Ochiai, Y. (2004) Primary structure and thermostability of bigeye tuna myoglobin in relation to those from other scombridae fish. *Fish. Sci.* **70**, 875–884
- Ueki, N., Chow, C.J., and Ochiai, Y. (2005) Characterization of bullet tuna myoglobin with reference to thermostability-structure relationship. *J. Agric. Food Chem.* **53**, 4968–4975
- Yang, J.T., Wu, C-S.C., and Martinez, H.M. (1986) Calculation of protein concentration from circular dichroism. *Methods Enzymol.* **130**, 208–269
- Ueki, N. and Ochiai, Y. (2005) Structural stabilities of recombinant scombridae fish myoglobins. *Biosci. Biotechnol. Biochem.* **69**, 1935–1943
- Chow, C.J. (1991) Relationship between the stability and autoxidation of myoglobin. *J. Agric. Food Chem.* **39**, 22–26
- Kyte, J. and Doolittle, R.F. (1982) A simple method for displaying the hydrophobic character of a protein. *J. Mol. Biol.* **157**, 105–132
- Munoz, V. and Serrano, L. (1997) Development of the multiple sequence approximation in the context of AGADIR's model of  $\alpha$ -helix formation. Comparison with the Lifson-Roig formalism. *Biopolymers* **41**, 495–509
- Thompson, J.D., Higgins, D.G., and Gibson, T.J. (1994) CLUSTAL W: improving the sensitivity of progressive multiple sequence alignment through sequence weighting, position-specific gap penalties and weight matrix choice. *Nucleic Acids Res.* **22**, 4673–4680
- Marcinek, D.J., Bonaventura, J., Wittenberg, J.B., and Block, B.A. (2001) Oxygen affinity and amino acid sequence of myoglobins from endothermic and ectothermic fish. *Am. J. Physiol. Regul. Integr. Comp. Physiol.* **280**, R1123–R1133
- Laemmli, U.K. (1970) Cleavage of structural proteins during the assembly of the head of bacteriophage T4. *Nature* **227**, 680–685
- Fontana, A., Zambonin, M., Polverino de Laureto, P., De Fillipis, V., Clementi, A., and Scaramella, E. (1997) Probing the conformational state of apomyoglobin by limited proteolysis. *J. Mol. Biol.* **266**, 223–230

28. Loh, S.N., Kay, M.S., and Baldwin, R.L. (1995) Structure and stability of a second molten globule intermediate in the apomyoglobin folding pathway. *Proc. Natl. Acad. Sci. USA* **92**, 5446–5450
29. Nishimura, C., Dysin, H.J., and Wright, P.E. (2006) Identification of native and non-native structure in kinetic folding intermediates of apomyoglobin. *J. Mol. Biol.* **355**, 139–156
30. Elizer, D., Jennings, P.A., Wright, P.E., Doniach, S., Hodgson, K.O., and Tsuruta, H. (1995) The radius of gyration of an apomyoglobin folding intermediate. *Science* **270**, 487–488
31. Dartigalongue, T. and Hache, F. (2006) Time-resolved circular dichroism in carbonmonoxy-myoglobin: The central role of the proximal histidine. *Chirality* **18**, 273–278
32. O'Neil, K.T. and DeGrado, W.F. (1990) A thermodynamic scale for the helix-forming tendencies of the commonly occurring amino acids. *Science* **250**, 646–651
33. Pace, C.N. and Scholtz, J.M. (1998) A helix propensity scale based on experimental studies of peptides and proteins. *Biophys. J.* **75**, 422–427
34. Vilasi, S., Dosi, R., Iannuzzi, C., Malmo, C., Parente, A., Irace, G., and Sirangelo, I. (2006) Kinetics of amyloid aggregation of mammal apomyoglobins and correlation with their amino acid sequences. *FEBS Lett.* **580**, 1681–1684
35. Isogai, Y. (2006) Native protein sequences are designed to destabilize folding intermediates. *Biochemistry* **45**, 2488–2492